Bulletin of Electrical Engineering and Informatics
Vol. 11, No. 1, February 2022, pp. 270∼277
ISSN: 2302-9285, DOI: 10.11591/eei.v11i1.3297

Ergodic capacity computation in cognitive radio aided non-orthogonal multiple access systems

Dinh-Thuan Do, Chi-Bao Le
Faculty of Electronics Technology, Industrial University of Ho Chi Minh City (IUH), Vietnam

Article Info

Article history:

Received Oct 30, 2020
Revised Jun 14, 2021
Accepted Dec 14, 2021

Keywords:

Cognitive radio
Ergodic capacity
Non-orthogonal multiple access

ABSTRACT

In this article, the performance of cognitive radio system benefits from non-orthogonal multiple access (NOMA) scheme. We then examine system metrics to adjust its quality of signal processing. We focus on performance of the secondary network containing NOMA users which have some impacts from normal user and primary nodes. We refer to enhancement of the fairness and spectrum utilization by enabling spectrum sharing. In particular, the NOMA power allocation factors are assigned to provide different ergodic capacities for two NOMA users in the downlink of such cognitive radio-non-orthogonal multiple access (CR-NOMA) system. This article presents approximated ergodic capacity of secondary users, in which this system adopts the Rayleigh fading. The closed-form expressions are expected to match with Monte-Carklo simulation results and main system parameters can be determined to control performance of such CR-NOMA. Finally, this system is prominent once its performance outperforms than that of conventional orthogonal multiple access (OMA)-based system.

Corresponding Author:

Dinh-Thuan Do
Faculty of Electronics Technology, Industrial University of Ho Chi Minh City (IUH)
12 Nguyn Văn Bo, Phng 4, Gò Vp, Thành ph H Chí Minh, Vietnam
Email: dodinhthuan@iuh.edu.vn

1. INTRODUCTION

To enhance the spectrum efficiency, CR is a promising technique to allocate the secondary users to access the licensed spectrum dynamically [1]–[3]. The strategies of underlay and/or overlay spectrum sharing are widely deployed to benefit CR scheme to emerging networks. To avoid collision with the primary network (PN) in the overlay strategy, the secondary users detect the underutilized licensed spectrum to access the PN [4]–[6]. In case of the underlay strategy, the licensed spectrum can be shared with the secondary network by managing the interfere to the primary receivers under a threshold [7]–[9].

Besides CR technique, NOMA technique can further improve the spectrum efficiency [10]–[15]. In the context of NOMA [16]–[21], the transmitters allocate different transmit power levels to multiple users to access on the same frequency. The receiver employing successive interference cancellation (SIC) to distinguish the different signals [22]. Thanks to benefits of both the CR and NOMA techniques, the CR-NOMA networks will not only increase the number of serving users and enhance the spectrum efficiency as well, which is a promising system for the 5th generation wireless networks [23]. Li *et al.* the authors [24] designed the relaying scheme employed in the secondary network of the considered CR-NOMA. In such, a relay is allowed to wireless power transfer to far users in the secondary network. Mu *et al.* in [25], by combining NOMA and CR network, such system provides to users a new era of reliable, seamless, and massive connectivity. In particular, this work studied the relay selection in CR-NOMA networks to achieve advantage of the spectrum sharing model.

The missing analysis in recent results in [24], [25] has motivated to consider ergodic capacity of CR-NOMA system.

The remaining parts of this article is summarized is being as. We describe scheme of CR-NOMA for signal processing at secondary users in section 2. We compute expressions of signal to interference plus noise ratio (SINR). The closed-form formula of ergodic capacity is presented in section 3 and then main simulation results are verified in section 4. In section 5, we provide some key findings to conclude the article.

2. SYSTEM MODEL

A CR-aided NOMA system is more important to examine its performance at secondary network (SN) in a downlink, as shown in Figure 1. Such SN includes of a secondary source (for example access point (AP)), two destination users (U1, U2), other cellular user equipment (CUE) as well as a primary destination (PD). The wireless channels in such CR-NOMA are adopted quasi-static independent but not identically distributed (i.i.n.d) Rayleigh fading. The links $AP \to PD$, $AP \to U_1$, $AP \to U_2$, $CUE \to U_1$ and $CUE \to U_2$ experience with coefficients as $h_{SP} \sim \mathcal{CN}(0, \lambda_{SP})$, $h_{AU_1} \sim \mathcal{CN}(0, \lambda_{AU_1})$, $h_{AU_2} \sim \mathcal{CN}(0, \lambda_{AU_2})$, $h_{CU_1} \sim \mathcal{CN}(0, \lambda_{CU_1})$ and $h_{CU_2} \sim \mathcal{CN}(0, \lambda_{CU_2})$, respectively.

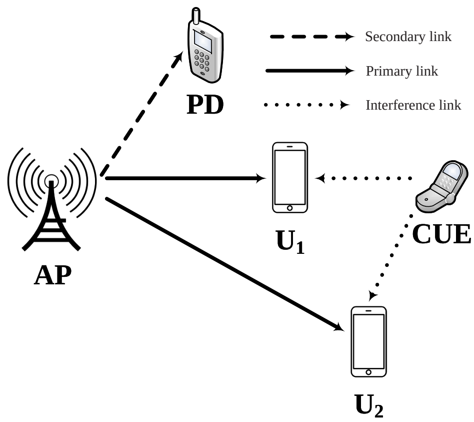

Figure 1. A sketch of of CR-aided NOMA system

In the considered system, the cognitive transmitter intends to send signals to the secondary destinations. To guarantee operation of primary network, the secondary source AP keeps the transmit power as the following constraint [26]:

$$P_{AP} = \min\left(\bar{P}_{AP}, \frac{Q}{|h_{SP}|^2}\right), \tag{1}$$

in which the secondary transmitter has $\bar{P}_{AP}$ as the maximum power. Of course, the transmit system is constrained by the interference at the primary receiver which is associated with threshold power of Q.

We call x_1, x_2 and x_CUE as the signals for U_1, U_2 and CUE, respectively. In NOMA, power allocation factors are a_1, a_2, and $a_1 < a_2$, $a_1 + a_2 = 1$. The received signals at the two users are given by:

$$y_{U_i} = h_{AU_i}\left[\sum_{j=1}^{2}\sqrt{a_j P_{AP}}x_j\right] + \sqrt{\kappa P_{CUE}}h_{CU_i}x_{CUE} + n_{U_i} \quad , i \in \{1, 2\}, \tag{2}$$

where κ, $0 \le \kappa \le 1$ represents for scaling factor related to interference, n_{U_i} is additive white Gaussian noise with mean power N_0, P_{AP} and P_{CUE} are the normalized transmission powers at the AP and CUE, respectively. h_{CU_i} is interference channel from the CUE to the users U_i and .

To further evaluate system performance, the SINR at user U_1 needs be computed. SINR at user U_1

treats signal from U_2 as noise, we have:

$$\tilde{\gamma}_{U_2 \to U_1} = \frac{\rho_{AP} a_2 |h_{AU_1}|^2}{a_1 \rho_{AP} |h_{AU_1}|^2 + \kappa \rho_{CUE} |h_{CU_1}|^2 + 1}, \tag{3}$$

where $\rho_{AP} = \frac{P_{AP}}{N_0}$ and $\rho_{CUE} = \frac{P_{CUE}}{N_0}$ are the transmit SNR at the AP and the CUE respectively.

By enabling SIC, we compute the SINR at U_1 by:

$$\tilde{\gamma}_{U_1} = \frac{a_1 \rho_{AP} |h_{AU_1}|^2}{\kappa \rho_{CUE} |h_{CU_1}|^2 + 1}. \tag{4}$$

To detect its own signal x_2, SINR at U_2 is given by:

$$\tilde{\gamma}_{U_2} = \frac{\rho_{AP} a_2 |h_{AU_2}|^2}{a_1 \rho_{AP} |h_{AU_2}|^2 + \kappa \rho_{CUE} |h_{CU_2}|^2 + 1}. \tag{5}$$

3. COMPUTATION OF ERGODIC CAPACITY

3.1. Ergodic capacity of U_1

By definition, we achieve ergodic capacity for user U_1 as:

$$\begin{aligned} C_{U_1} =& \frac{1}{2} E\left\{ \log\left(1 + \tilde{\gamma}_{U_1}\right)\right\} \\ =& \frac{1}{2} E\left\{ \log\left(1 + \underbrace{\frac{a_1 \rho_{AP} |h_{AU_1}|^2}{\kappa \rho_{CUE} |h_{CU_1}|^2 + 1}}_{X}\right)\right\} \\ =& \frac{1}{2\ln 2} \int\limits_0^\infty \frac{1 - F_X(x)}{1 + x} dx. \end{aligned} \tag{6}$$

It is noted that $F_X(x)$ is written by:

$$\begin{aligned} F_X(x) =& 1 - \Pr\left(|h_{AU_1}|^2 > \frac{x}{a_1 \bar{\rho}_{AP}} \left(\kappa \rho_{CUE} |h_{CU_1}|^2 + 1 \right), |h_{SP}|^2 < \frac{\rho_Q}{\bar{\rho}_{AP}} \right) \\ & - \Pr\left(|h_{AU_1}|^2 > \frac{x}{a_1 \rho_Q} \left(\kappa \rho_{CUE} |h_{CU_1}|^2 |h_{SP}|^2 + |h_{SP}|^2 \right), |h_{SP}|^2 > \frac{\rho_Q}{\bar{\rho}_{AP}} \right) \\ =& 1 - \int\limits_0^{\frac{\rho_Q}{\bar{\rho}_{AP}}} f_{|h_{SP}|^2}(y) \int\limits_0^\infty f_{|h_{CU_1}|^2}(z) \left[1 - F_{|h_{AU_1}|^2}\left(\frac{x\left(\kappa \rho_{CUE} z + 1\right)}{a_1 \bar{\rho}_{AP}} \right) \right] dy dz \\ & - \int\limits_{\frac{\rho_Q}{\bar{\rho}_{AP}}}^\infty f_{|h_{SP}|^2}(y) \int\limits_0^\infty f_{|h_{CU_1}|^2}(z) \left[1 - F_{|h_{AU_1}|^2}\left(\frac{x\left(\kappa \rho_{CUE} z y + y\right)}{a_1 \rho_Q} \right) \right] dy dz \\ =& 1 - \left(1 - e^{-\frac{\rho_Q}{\bar{\rho}_{AP} \lambda_{SP}}} \right) \frac{e^{-\frac{x}{\eta \bar{\rho}_{AP}}}}{\lambda_{CU_1}} \int\limits_0^\infty e^{-z\left(\frac{1}{\lambda_{CU_1}} + \frac{\kappa \rho_{CUE} x}{\eta \bar{\rho}_{AP}} \right)} dz \\ & - \frac{1}{\lambda_{SP} \lambda_{CU_1}} \int\limits_{\frac{\rho_Q}{\bar{\rho}_{AP}}}^\infty e^{-y\left(\frac{1}{\lambda_{SP}} + \frac{x}{\eta \rho_Q} \right)} \int\limits_0^\infty e^{-z\left(\frac{1}{\lambda_{CU_1}} + \frac{\kappa \rho_{CUE} y x}{\eta \rho_Q} \right)} dy dz \\ =& 1 - \left(1 - e^{-\frac{\rho_Q}{\bar{\rho}_{AP} \lambda_{SP}}} \right) \frac{\eta \bar{\rho}_{AP} e^{-\frac{x}{\eta \bar{\rho}_{AP}}}}{\left(\eta \bar{\rho}_{AP} + \nu x \right)} - \frac{\eta \rho_Q}{\lambda_{SP} \nu x} \int\limits_{\frac{\rho_Q}{\bar{\rho}_{AP}}}^\infty \frac{e^{-y\left(\frac{1}{\lambda_{SP}} + \frac{x}{\eta \rho_Q} \right)}}{\left[\frac{\eta \rho_Q}{\nu x} + y \right]}, \end{aligned} \tag{7}$$

where $\eta = \lambda_{AU_1} a_1$ and $\nu = \lambda_{CU_1} \kappa \rho_{CUE}$.

We using [[27], (3.352.2)] $F_X(x)$ is given as:

$$\begin{aligned} F_X(x) =& 1 - \left(1 - e^{-\frac{\rho_Q}{\bar{\rho}_{AP}\lambda_{SP}}}\right) \frac{\eta\bar{\rho}_{AP} e^{-\frac{x}{\eta\bar{\rho}_{AP}}}}{[\eta\bar{\rho}_{AP} + \nu x]} \\ &+ \frac{\eta\rho_Q}{\lambda_{SP}\nu x} e^{\frac{\eta\rho_Q}{\nu x}\left(\frac{1}{\lambda_{SP}} + \frac{x}{\eta\rho_Q}\right)} Ei\left(-\left(\frac{1}{\lambda_{SP}} + \frac{x}{\eta\rho_Q}\right)\left(\frac{\rho_Q}{\bar{\rho}_{AP}} + \frac{\eta\rho_Q}{\nu x}\right)\right). \end{aligned} \tag{8}$$

Substituting (8) into (6), C_{U_1} is given as:

$$\begin{aligned} C_{U_1} =& \frac{1}{2\ln 2} \int_0^{\frac{a_2}{a_1}} \frac{1}{1+x} (1 - F_X(x)) dx \\ =& \frac{1}{2\ln 2} \int_0^{\infty} \frac{1}{1+x} \left[\left(1 - e^{-\frac{\rho_Q}{\bar{\rho}_{AP}\lambda_{SP}}}\right) \frac{\eta\bar{\rho}_{AP} e^{-\frac{x}{\eta\bar{\rho}_{AP}}}}{(\eta\bar{\rho}_{AP} + \nu x)} \right. \\ &\left. - \frac{\eta\rho_Q}{\lambda_{SP}\nu x} e^{\frac{\eta\rho_Q}{\nu x}\left(\frac{1}{\lambda_{SP}} + \frac{x}{\eta\rho_Q}\right)} Ei\left(-\left(\frac{1}{\lambda_{SP}} + \frac{x}{\eta\rho_Q}\right)\left(\frac{\rho_Q}{\bar{\rho}_{AP}} + \frac{\eta\rho_Q}{\nu x}\right)\right)\right] dx. \end{aligned} \tag{9}$$

Let $t = \frac{4}{\pi} \arctan(x) - 1 \Rightarrow \tan\left(\frac{\pi(t+1)}{4}\right) = x \Rightarrow \frac{\pi}{4}\sec^2\left(\frac{\pi}{4}(t+1)\right) dt = dx$, C_{U_1} is given by:

$$\begin{aligned} C_{U_1} =& \frac{\pi}{8\ln 2} \int_{-1}^{1} \frac{\sec^2\left(\frac{\pi}{4}(t+1)\right)}{1+\ell(t)} \left[\left(1 - e^{-\frac{\rho_Q}{\bar{\rho}_{AP}\lambda_{SP}}}\right) \frac{\eta\bar{\rho}_{AP} e^{-\frac{\ell(t)}{\eta\bar{\rho}_{AP}}}}{(\eta\bar{\rho}_{AP} + \nu\ell(t))} \right. \\ &\left. - \frac{\eta\rho_Q}{\lambda_{SP}\nu\ell(t)} e^{\frac{\eta\rho_Q}{\nu\ell(t)}\left(\frac{1}{\lambda_{SP}} + \frac{\ell(t)}{\eta\rho_Q}\right)} Ei\left(-\left(\frac{1}{\lambda_{SP}} + \frac{\ell(t)}{\eta\rho_Q}\right)\left(\frac{\rho_Q}{\bar{\rho}_{AP}} + \frac{\eta\rho_Q}{\nu\ell(t)}\right)\right)\right] dt. \end{aligned} \tag{10}$$

where $\ell(t) = \tan\left(\frac{\pi(t+1)}{4}\right)$.

Unfortunately, deriving a closed-form expression for (10) is difficult task, we can obtain accurate approximation. We have new result using Gaussian-Chebyshev quadrature [[28] (25.4.38)].

$$\begin{aligned} C_{U_1} \approx& \frac{\pi^2}{8T\ln 2} \sum_{t=1}^{T} \frac{\sqrt{1-\varphi_t^2}}{1+\ell(\varphi_t)} \sec^2\left(\frac{\pi}{4}(\varphi_t + 1)\right) \left[\left(1 - e^{-\frac{\rho_Q}{\bar{\rho}_{AP}\lambda_{SP}}}\right) \frac{\eta\bar{\rho}_{AP} e^{-\frac{\ell(\varphi_t)}{\eta\bar{\rho}_{AP}}}}{(\eta\bar{\rho}_{AP} + \nu\ell(\varphi_t))} \right. \\ &\left. - \frac{\eta\rho_Q}{\lambda_{SP}\nu\ell(\varphi_t)} e^{\frac{\eta\rho_Q}{\nu\ell(\varphi_t)}\left(\frac{1}{\lambda_{SP}} + \frac{\ell(\varphi_t)}{\eta\rho_Q}\right)} Ei\left(-\left(\frac{1}{\lambda_{SP}} + \frac{\ell(\varphi_t)}{\eta\rho_Q}\right)\left(\frac{\rho_Q}{\bar{\rho}_{AP}} + \frac{\eta\rho_Q}{\nu\ell(\varphi_t)}\right)\right)\right], \end{aligned} \tag{11}$$

where $\varphi_t = \cos\left(\frac{2t-1}{2T}\pi\right)$.

3.2. Ergodic capacity of U_2

Similarly as computation for U_1, the ergodic capacity for U_2 is formulated by:

$$C_{U_2} = \frac{1}{2} E\left\{\log\left(1 + \tilde{\gamma}_{U_2}\right)\right\} = \frac{1}{2\ln 2} \int_0^{\frac{a_2}{a_1}} \frac{1}{1+x} \bar{F}_{|h_{AU_2}|^2}\left(\frac{x}{a_2 - a_1 x}\right) dx, \tag{12}$$

in which $\bar{F}_{|h_{AU_2}|^2}(x) = 1 - F_{|h_{AU_2}|^2}(x)$ denotes the complementary CDF of $|h_{AU_2}|^2$. We continue to have $F_{|h_{AU_2}|^2}(x)$ which is similar as (8).

$$F_{|h_{AU_2}|^2}(x) = \left[\left(1 - e^{-\frac{\rho_Q}{\lambda_{SP}\bar{\rho}_{AP}}}\right) \frac{\lambda_{AU_2} e^{-\frac{x}{\lambda_{AU_2}\bar{\rho}_{AP}[a_2 - a_1 x]}}}{\left(\lambda_{AU_2} + \lambda_{CU_2}\kappa \frac{\rho_{CUE} x}{\bar{\rho}_{AP}[a_2 - a_1 x]}\right)} \right.$$
$$+ \frac{\rho_Q [a_2 - a_1 x] \lambda_{AU_2}}{\lambda_{SP}\lambda_{CU_2}\kappa\rho_{CUE} x} e^{\frac{\rho_Q[a_2 - a_1 x]\lambda_{AU_2}}{\lambda_{CU_2}\kappa\rho_{CUE} x}\left(\frac{1}{\lambda_{SP}} + \frac{x}{\rho_Q \lambda_{AU_2}[a_2 - a_1 x]}\right)} \tag{13}$$
$$\left. \times Ei\left(-\left(\frac{1}{\lambda_{SP}} + \frac{x}{\rho_Q \lambda_{AU_2}[a_2 - a_1 x]}\right)\left(\frac{\rho_Q}{\bar{\rho}_{AP}} + \frac{\rho_Q [a_2 - a_1 x] \lambda_{AU_2}}{\lambda_{CU_2}\kappa\rho_{CUE} x}\right)\right)\right].$$

Substituting (13) into (12), C_{U_2} is calculated as:

$$C_{U_2} = \frac{1}{2\ln 2} \int_0^{\frac{a_2}{a_1}} \frac{1}{1+x} \left[\left(1 - e^{-\frac{\rho_Q}{\lambda_{SP}\bar{\rho}_{AP}}}\right) \frac{\lambda_{AU_2} e^{-\frac{\bar{\delta}_{AP}(x)}{\lambda_{AU_2}}}}{\left(\lambda_{AU_2} + \lambda_{CU_2}\kappa\rho_{CUE}\bar{\delta}_{AP}(x)\right)} \right.$$
$$\left. - \frac{\vartheta(x)}{\lambda_{SP}} e^{\vartheta(x)\left(\frac{1}{\lambda_{SP}} + \frac{\tilde{\delta}_Q(x)}{\lambda_{AU_2}}\right)} Ei\left(-\left(\frac{1}{\lambda_{SP}} + \frac{\tilde{\delta}_Q(x)}{\lambda_{AU_2}}\right)\left(\frac{\rho_Q}{\bar{\rho}_{AP}} + \vartheta(x)\right)\right)\right] dx, \tag{14}$$

where $\bar{\delta}_{AP}(x) = \frac{x}{\bar{\rho}_{AP}[a_2 - a_1 x]}$, $\tilde{\delta}_Q(x) = \frac{x}{\rho_Q [a_2 - a_1 x]}$ and $\vartheta(x) = \frac{\lambda_{AU_2}}{\lambda_{CU_2}\kappa\rho_{CUE}\tilde{\delta}_Q(x)}$.

Although, achieving a closed-form expression for (14) is tough task, an accurate approximation could be considered by employing Gaussian-Chebyshev quadrature [[27] (25.4.38)], C_{U_2} is given by:

$$C_{U_2} \approx \frac{\pi a_2}{2K\ln 2} \sum_{k=1}^{K} \frac{\sqrt{1-\phi_k^2}}{2a_1 + a_2(\phi_k + 1)} \left[\left(1 - e^{-\frac{\rho_Q}{\lambda_{SP}\bar{\rho}_{AP}}}\right) \frac{\lambda_{AU_2} e^{-\frac{\Delta(\phi_k)}{\lambda_{AU_2}}}}{\left(\lambda_{AU_2} + \lambda_{CU_2}\kappa\rho_{CUE}\Delta(\phi_k)\right)} \right.$$
$$\left. - \frac{\vartheta(\phi_k)}{\lambda_{SP}} e^{\vartheta(\phi_k)\left(\frac{1}{\lambda_{SP}} + \frac{\Theta(\phi_k)}{\lambda_{AU_2}}\right)} Ei\left(-\left(\frac{1}{\lambda_{SP}} + \frac{\Theta(\phi_k)}{\lambda_{AU_2}}\right)\left(\frac{\rho_Q}{\bar{\rho}_{AP}} + \vartheta(\phi_k)\right)\right)\right], \tag{15}$$

where $\phi_k = \cos\left(\frac{2k-1}{2K}\pi\right)$, $\Delta(x) = \frac{a_2(t+1)}{\bar{\rho}_{AP} a_1 [a_2(1-t)]}$, $\Theta(x) = \frac{a_2(t+1)}{\rho_Q a_1 [a_2(1-t)]}$ and $\vartheta(x) = \frac{\lambda_{AU_2}}{\lambda_{CU_2}\kappa\rho_{CUE}\Theta(x)}$.

4. SIMULATION RESULTS AND DISCUSSION

To verify closed-form expressions, we set power factor $a_2 = 0.9$. The wireless channels are characterized as $\lambda_{SP} = d_0^{-\beta}$, $\lambda_{AU_1} = d_1^{-\beta}$, $\lambda_{AU_2} = (1 - U_1)^{-\beta}$, $\lambda_{CU_1} = d_{CU_1}^{-\beta}$ and $\lambda_{CU_2} = d_{CU_2}^{-\beta}$, along with distances are $d_0 = 0.1$, $d_1 = 0.3$, $d_{CU_1} = 0.3$ and $d_{CU_2} = 0.7$, path-loss exponent is $\beta = 2$. Although depending on service required, data rates should be $R_1 = 1$ and $R_2 = 0.5$. We set SNR of interference from primary network $\rho_Q = 30\,dB$. To obtain a close approximation, the Gauss-Chebyshev parameter could be $T = K = 20$.

Figures 2-4 exhibit ergodic capacity for considered CR-NOMA. We can see the trend of curves in term of ergodic capacity with different values of κ for Figure 2. Especially in Figure 3, at fixed value of ρ_Q, the ergodic capacity only increase at lower range of ρ_Q, after the point $\rho_Q = 35$, the ergodic capacity keeps unchanged.

In Figure 3, higher power of interference from the CUE is main reason to make ergodic capacity of two users reduce. It can be seen ergodic capacity of two users are low at high region of κ. Figure 5 confirms that CR system relying NOMA outperforms than that using OMA scheme.

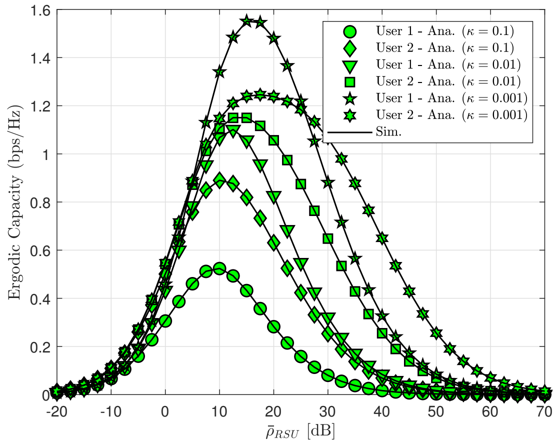

Figure 2. Ergodic capacity versus transmit SNR at the RSU

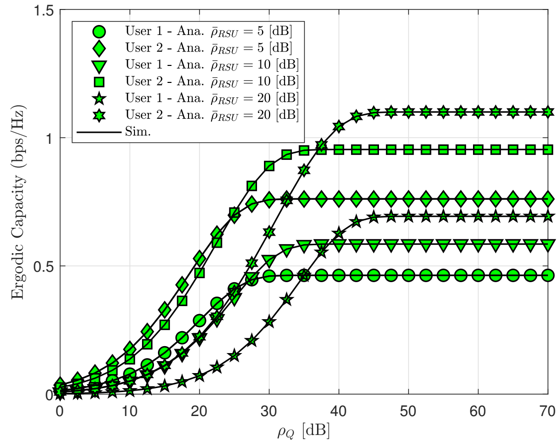

Figure 3. Ergodic capacity versus transmit SNR at the primary node, with $\kappa = 0.1$

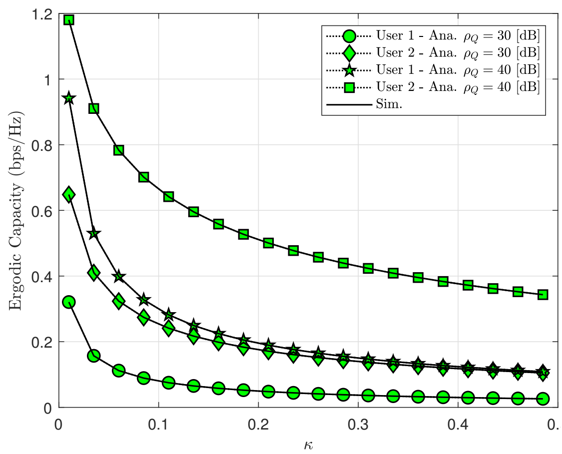

Figure 4. Ergodic capacity versus κ, with $\bar{\rho}_{RSU} = 30$ [dB]

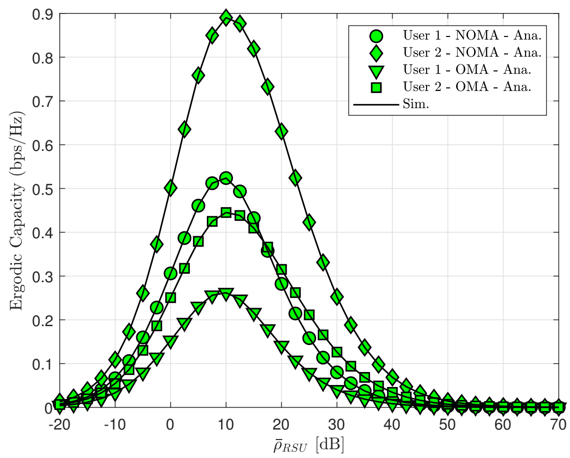

Figure 5. Comparison between CR scheme with OMA and with NOMA, with $\kappa = 0.1$ and $\rho_Q = 30$ [dB]

5. CONCLUSION

In this paper, we have evaluated performance of underlay CR-NOMA network by introducing the closed-form expressions of ergodic capacity under Rayleigh fading. We can confirm exactness of the derived closed-form expressions by numerical results, and the ergodic capacity of CR-NOMA and CR-OMA were compared. The proposed CR-NOMA can improve ergodic capacity at high region of transmit SNR at the secondary source. Moreover, the numerical results showed that the different power allocation factors lead to performance gap among two users and the performance fairness is achieved for both users.

REFERENCES

[1] X. Chen, H.-H. Chen, and W. Meng, “Cooperative communications for cognitive radio networks—From theory to applications,” in *IEEE Communications Surveys Tutorials*, vol. 16, no. 3, pp. 1180-1192, 2014, doi: 10.1109/SURV.2014.021414.00066.

[2] I. Kakalou, K. E. Psannis, P. Krawiec, and R. Badea, “Cognitive radio network and network service chaining toward 5G: Challenges and requirements,” in *IEEE Communications Magazine*, vol. 55, no. 11, pp. 145-151, November 2017, doi: 10.1109/MCOM.2017.1700086.

[3] Dinh-Thuan Do and A.-T. Le, “NOMA based cognitive relaying: Transceiver hardware impairments, relay selection policies and outage performance comparison,” *Computer Communications*, vol. 146, pp. 144-154, October 2019, doi: 10.1016/j.comcom.2019.07.023.

[4] H. Zhang, C. Jiang, X. Mao, and H. H. Chen, "Interference-limited resource optimization in cognitive femtocells with fairness and imperfect spectrum sensing," in *IEEE Transactions on Vehicular Technology*, vol. 65, no. 3, pp. 1761-1771, March 2016, doi: 10.1109/TVT.2015.2405538.

[5] H. Zhang, Y. Nie, J. Cheng, V. C. M. Leung, and A. Nallanathan, "Sensing time optimization and power control for energy efficient cognitive small cell with imperfect hybrid spectrum sensing," in *IEEE Transactions on Wireless Communications*, vol. 16, no. 2, pp. 730-743, February 2017, doi: 10.1109/TWC.2016.2628821.

[6] W. Liang, S. X. Ng, and L. Hanzo, "Cooperative overlay spectrum access in cognitive radio networks," in *EEE Communications Surveys Tutorials*, vol. 19, no. 3, pp. 1924-1944, thirdquarter 2017, doi: 10.1109/COMST.2017.2690866.

[7] F. Jasbi and D. K. C. So, "Hybrid overlay/underlay cognitive radio network with MC-CDMA," in *IEEE Transactions on Vehicular Technology*, vol. 65, no. 4, pp. 2038–2047, April 2016, doi: 10.1109/TVT.2015.2417195.

[8] B. Kumar and S. Prakriya, "Performance of adaptive link selection with buffer-aided relays in underlay cognitive networks," *IEEE Transactions on Vehicular Technology*, vol. 67, no. 2, pp. 1492–1509, February 2018, doi: 10.1109/TVT.2017.2761990.

[9] S. Dadallage, C. Yi, and J. Cai, "Joint beamforming, power, and channel allocation in multiuser and multichannel underlay MISO cognitive radio networks," in *IEEE Transactions on Vehicular Technology*, vol. 65, no. 5, pp. 3349–3359, May 2016, , doi: 10.1109/TVT.2015.2440412.

[10] Z. Ding, *et al.*, "Application of non-orthogonal multiple access in LTE and 5G networks," in *IEEE Communications Magazine*, vol. 55, no. 2, pp. 185-191, February 2017, doi: 10.1109/MCOM.2017.1500657CM.

[11] Z. Ding, X. Lei, G. K. Karagiannidis, R. Schober, J. Yuan, and V. K. Bhargava, "A survey on non-orthogonal multiple access for 5G networks: Research challenges and future trends," in *IEEE Journal on Selected Areas in Communications*, vol. 35, no. 10, pp. 2181-2195, October 2017, doi: 10.1109/JSAC.2017.2725519.

[12] Dinh-Thuan Do, M.-S. Van Nguyen, T.-A. Hoang, and B. M. Lee, "Exploiting Joint Base Station Equipped Multiple Antenna and Full-Duplex D2D Users in Power Domain Division Based Multiple Access Networks," *Sensors*, vol. 19, no. 11, p. 2475, 2019, doi: 10.3390/s19112475.

[13] Dinh-Thuan Do, A.-T. Le, Chi-Bao Le, and B. M. Lee "On Exact Outage and Throughput Performance of Cognitive Radio based Non-Orthogonal Multiple Access Networks With and Without D2D Link," *Sensors*, vol. 19, no. 15, p. 3314, 2019, doi: 10.3390/s19153314.

[14] Dinh-Thuan Do, Chi-Bao Le, and A.-T. Le, "Cooperative underlay cognitive radio assisted NOMA: secondary network improvement and outage performance, " *TELKOMNIKA Telecommunication Computing Electronics and Control*, vol. 17, no. 5, pp. 2147-2154, October 2019, doi: 10.12928/TELKOMNIKA.v17i5.12451.

[15] Dinh-Thuan Do and T.-T. Thi Nguyen, "Exact Outage Performance Analysis of Amplify-and Forward-Aware Cooperative NOMA," *TELKOMNIKA Telecommunication Computing Electronics and Control*, vol. 16, no. 5, pp. 1966-1973, October 2018, doi: 10.12928/TELKOMNIKA.v16i5.9823.

[16] X. Li, Q. Wang, Y. Liu, T. A. Tsiftsis, Z. Ding, and A. Nallanathan, "UAV-Aided Multi-Way NOMA Networks with Residual Hardware Impairments," in *IEEE Wireless Communications Letters*, vol. 9, no. 9, pp. 1538-1542, September 2020, doi: 10.1109/LWC.2020.2996782.

[17] X. Li, *et al.*, "Cooperative Wireless-Powered NOMA Relaying for B5G IoT Networks with Hardware Impairments and Channel Estimation Errors, " in *IEEE Internet of Things Journal*, vol. 8, no. 7, pp. 5453-5467, April 2021, doi: 10.1109/JIOT.2020.3029754.

[18] Z. Ding and H. V. Poor, "A simple design of IRS-NOMA transmission," in *IEEE Communications Letters*, vol. 24, no. 5, pp. 1119-1123, May 2020, doi: 10.1109/LCOMM.2020.2974196.

[19] G. Yang, X. Xu, and Y. Liang, "Intelligent reflecting surface assisted non-orthogonal multiple access," *2020 IEEE Wireless Communications and Networking Conference (WCNC)*, 2020, pp. 1-6, doi: 10.1109/WCNC45663.2020.9120476.

[20] I. Budhiraja, N. Kumar, S. Tyagi, S. Tanwar, and M. S. Obaidat, "URJA: Usage Jammer as a Resource Allocation for Secure Transmission in a CR-NOMA-Based 5G Femtocell System," *IEEE Systems Journal*, vol. 15, no. 2, pp. 1776-1785, June 2021, doi: 10.1109/JSYST.2020.2999474.

[21] W. Zhao, R. She, and H. Bao, "Energy Efficiency Maximization for Two-Way Relay Assisted CR-NOMA System Based on SWIPT," in *IEEE Access*, vol. 7, pp. 72062-72071, 2019, doi: 10.1109/ACCESS.2019.2919965.

[22] F. Fang, H. Zhang, J. Cheng, S. Roy, and V. C. M. Leung, "Joint user scheduling and power allocation optimization for energy-efficient NOMA systems with imperfect CSI," in *IEEE Journal on Selected Areas in Communications*, vol. 35, no. 12, pp. 2874-2885, December 2017, doi: 10.1109/JSAC.2017.2777672.

[23] F. Zhou, Y. Wu, Y.-C. Liang, Z. Li, Y. Wang, and K.-K. Wong, "State of the art, taxonomy, and open issues on cognitive radio networks with NOMA," in *IEEE Wireless Communications*, vol. 25, no. 2, pp. 100-108, April 2018, doi: 10.1109/MWC.2018.1700113.

[24] Y. Li, M. Jiang, Q. Zhang, and J. Qin, "Joint beamforming design in multi-cluster MISO NOMA reconfigurable intelligent surface-aided downlink communication networks," in *IEEE Transactions on Communications*, vol. 69, no. 1, pp. 664-674, January 2021, doi: 10.1109/TCOMM.2020.3032695.

[25] X. Mu, Y. Liu, L. Guo, J. Lin, and N. Al-Dhahir, "Exploiting intelligent reflecting surfaces in NOMA networks: Joint beamforming optimization," in *IEEE Transactions on Wireless Communications*, vol. 19, no. 10, pp. 6884-6898, October 2020, doi: 10.1109/TWC.2020.3006915.

[26] S. Arzykulov, T. A. Tsiftsis, G. Nauryzbayev, and M. Abdallah, "Outage Performance of Cooperative Underlay CR-NOMA with Imperfect CSI," in *IEEE Communications Letters*, vol. 23, no. 1, pp. 176-179, Jan. 2019, doi: 10.1109/LCOMM.2018.2878730.

[27] M. Abramowitz and I. A. Stegun, "Handbook of Mathematical Functions with Formulas, Graphs, and Mathematical Table," New York, NY, USA: Dover, 1972.

[28] I. S. Gradshteyn and I. M. Ryzhik, *Table of Integrals, Series and Products*, 6th ed. New York, NY, USA: Academic Press, 2000.

BIOGRAPHIES OF AUTHORS

Dinh-Thuan Do (Senior Member, IEEE) received the B.S., M.Eng., and Ph.D. degrees in communications engineering from Vietnam National University (VNU-HCM), in 2003, 2007, and 2013, respectively. His research interests include signal processing in wireless communications networks, cooperative communications, nonorthogonal multiple access, full-duplex transmission, and energy harvesting. He was a recipient of the Golden Globe Award from the Vietnam Ministry of Science and Technology, in 2015 (Top ten excellent young scientists nationwide). He has served as a guest editor for eight prominent SCIE journals. He is currently serving as an associate editor for six journals, including EURASIP Journal on Wireless Communications and Networking, Computer Communications (Elsevier), and KSII Transactions on Internet and Information Systems. He can be contacted at email: dodinhthuan@iuh.edu.vn.

Chi-Bao Le was born in Binh Thuan, Vietnam. He is currently pursuing the master's degree in wireless communications. He has worked closely with Dr. Thuan at the Wireless Communications and Signal Processing Research Group, Industrial University of Ho Chi Minh City, Vietnam. His research interests include electronic design, signal processing in wireless communications networks, non-orthogonal multiple access, and physical layer security. He can be contacted at email: lechibao@iuh.edu.vn.